Earth and Planetary Science Letters 298 (2010) 361–366

Contents lists available at ScienceDirect

Earth and Planetary Science Letters

journal homepage: www.elsevier.com/locate/epsl

Shear wave anisotropy of textured hcp-Fe in the Earth's inner core

Jung-Fu Lin [a,*], Zhu Mao [a], Hasan Yavaş [b,c], Jiyong Zhao [b], Leonid Dubrovinsky [d]

[a] Department of Geological Sciences, Jackson School of Geosciences, The University of Texas at Austin, Austin, TX 78712, USA
[b] Advanced Photon Source, Argonne National Laboratory, Argonne, IL 60439, USA
[c] Department of Geology, The University of Illinois at Urbana–Champaign, Urbana, IL 61801, USA
[d] Bayerisches Geoinstitut, Universität Bayreuth, D-95440 Bayreuth, Germany

ARTICLE INFO

Article history:
Received 21 March 2010
Received in revised form 22 July 2010
Accepted 9 August 2010

Editor: L. Stixrude

Keywords:
Earth's inner core
elastic properties
iron
seismology
high pressure

ABSTRACT

Many seismological studies have confirmed that Vp travels 3–4% faster along the rotation axis of the Earth than along the equatorial plane in the inner core, indicating that the inner core is elastically anisotropic. However, seismic and mineral physics observations of the polarized Vs are still emerging. Thus far, the Vs anisotropy of the constitute iron crystals at relevant pressures of the Earth's core has remained mostly theoretical mainly because of the technical difficulties involved in measuring reliable Vs velocities of iron crystals. Here we have measured azimuthal Vs anisotropy of highly textured hcp-Fe at high pressures using nuclear resonant inelastic X-ray scattering, a technique sensitive to Vs, in a diamond anvil cell. Our results show that the azimuthal Vs is 2–4% faster along the crystallographic *c* axis than along the *a* axis at 158 GPa and 172 GPa. If one describes the Vp anisotropy of the inner core as a result of the textured hcp-Fe crystals, it is conceivable that azimuthal and polarized Vs anisotropies with a magnitude of a few percent also exist in the region. Since Vp and Vs of candidate iron phases behave quite differently in theoretical predictions, our results here indicate that future seismic observations of the Vs and Vp anisotropies of the inner core thus hold the key to deciphering the causes for the seismic and dynamic signatures as well as constitute iron phase(s) of the region.

Published by Elsevier B.V.

1. Introduction

Intriguing yet enigmatic phenomena of the Earth's inner core have recently been reported by deep-Earth seismology, geodynamics, and mineral physics studies including the compressional wave (Vp) anisotropy (Morelli et al., 1986; Woodhouse et al., 1986; Song and Helmburger, 1993; Tromp, 1993; Stixrude and Cohen, 1995; Song and Helmberger, 1998; Beghein and Trampert, 2003; Deuss, 2008), the differential super-rotation (Creager, 1997), the fine-scale seismic heterogeneity (Creager, 1997; Ishii and Dziewonski, 2002; Niu and Chen, 2008), the low rigidity and shear wave velocity (Vs) (Cao et al., 2005; Belonoshko et al., 2007, 2008; Wookey and Helffrich, 2008; Cao and Romanowicz, 2009), and the existence of iron crystals with textures in the inner core (Mao et al., 1998; Steinle-Neumann et al., 2001; Antonangeli et al., 2004; Vocadlo et al., 2003, 2009; Vocadlo, 2007; Dubrovinsky et al., 2007; Belonoshko et al., 2007, 2008). Particularly, Earth's inner core is known to be elastically anisotropic from many seismic analyses of the depth and directional dependence of the Vp (e.g., Morelli et al., 1986; Woodhouse et al., 1986). The Vp anisotropy of the innermost inner core also differs from that of the top of the inner core, with the slowest direction tilted at an angle of 45° to the equatorial plane, indicating the existence of seismic layering and a possible phase transition of the constitute iron alloy in the region (Creager, 1997; Ishii and Dziewonski, 2002; Niu and Chen, 2008; Vocadlo et al., 2009). It is mostly believed that such anisotropy can be explained by the preferred lattice orientation of the iron alloy crystals, although the underlying mechanisms for generating the texture and the degree of texturing all remain to be reconciled (Mao et al., 1998; Steinle-Neumann et al., 2001; Antonangeli et al., 2004; Vocadlo et al., 2003, 2009; Dubrovinsky et al., 2007). In a textured and elastically anisotropic inner core, two types of Vs anisotropies are to be expected: (1). azimuthal anisotropy in which Vs varies in different directions; (2). polarization anisotropy in which Vs is split into two waves, Vs_1 and Vs_2, with orthogonal polarizations that travel at different speeds. From an analysis of timing, amplitude and waveform of the seismic 'PKJKP' phase, a possible Vs splitting with approximately 1% in polarization anisotropy has been suggested for the inner core (Wookey and Helffrich, 2008).

Earth's inner core is mainly made of iron with a few percent of nickel, together with a small amount of light elements (see Li and Fei (2003) and Dubrovinsky and Lin (2009) for recent reviews). hcp-Fe crystals, widely believed to exist in the inner core (Takahashi and Bassett, 1964; Mao et al., 1990; Hemley and Mao, 2001), display strong lattice preferred orientations (textures), with *c* axes parallel to the compression axis of the high-pressure DAC (Mao et al., 1998; Wenk et al., 2000). Such stress-induced lattice strains with textures

* Corresponding author. Tel.: +1 512 471 8054.
E-mail address: afu@jsg.utexas.edu (J.-F. Lin).

0012-821X/$ – see front matter. Published by Elsevier B.V.
doi:10.1016/j.epsl.2010.08.006

have been measured using radial X-ray diffraction (RXD) to investigate elasticity on textured hcp-Fe crystals up to 211 GPa at room temperature (Mao et al., 1998), but the finite-strain theory and iso-stress assumptions used in the modeling, together with plastic deformation of the crystals, cast serious doubt on the reliability of the results (Antonangeli et al., 2006). Thus far, the Vs anisotropy of the hcp-Fe at relevant pressures of the Earth's core remains mostly theoretical, with studies predicting various degrees of the polarized and azimuthal Vs anisotropies along different orientations (e.g., Stixrude and Cohen, 1995; Laio et al., 2000; Steinle-Neumann et al., 2001; Vocadlo et al., 2003, 2009; Vocadlo, 2007; Sha and Cohen, 2010). Here we present new experimental results for the azimuthal Vs anisotropy of textured hcp-Fe crystals using nuclear resonant inelastic X-ray scattering (NRIXS), a technique sensitive to Vs, in a high-pressure diamond anvil cell (DAC).

2. Materials and experiments

^{57}Fe-enriched bcc-Fe starting sample (>95% enrichment) was purchased from Cambridge Isotope Laboratories, Inc., and was examined by X-ray diffraction and electron microprobe for its crystal structure and chemical composition. We used a Be gasket and a cubic BN gasket insert to contain the Fe sample at high pressures (Lin et al., 2008). The use of the ultrapure Be gasket (IF-1 grade), purchased from Bruch Wellman of the Electrofusion Products (Lin et al., 2010), was critical in the success of the experiments as it contained less than 0.03% iron impurity in which ^{57}Fe isotopes contributed negligibly to the measured energy spectra of the sample. The ultrapure Be gasket, however, was extremely brittle and required a tailored fit, pre-drilled hole in order to reach high pressures in a DAC. The cubic BN gasket insert with high strength allowed us to prepare samples with sufficient thickness for the experiments at unprecedented pressures (Fig. 1).

High-pressure NRIXS experiments were conducted using a high-resolution monochromator with 1 meV energy bandwidth at sector 3 of the Advanced Photon Source (APS), Argonne National Laboratory (ANL) (Sturhahn, 2004) (Fig. 1). Beveled diamond anvils of 100–300 or 60–180–300 μm in diameter were used with an ultrapure Be gasket 2 mm in diameter and 250 μm thick, together with a cubic BN gasket insert to contain ^{57}Fe-enriched sample of ~35 μm in diameter in a DAC. The samples were then compressed to 158 GPa (with culets of 100–300 μm) and 172 GPa (with culets of 60–180–300 μm) to convert them to textured hcp-Fe crystals. Previous studies with a similar sample preparation procedure have shown that non-hydrostatically compressed hcp-Fe crystals exhibit strong preferred orientations at such pressures (Singh et al., 1998; Mao et al., 1998; Wenk et al., 2000).

X-ray diffraction patterns were used to determine densities and pressures *in situ*, whereas RXD patterns revealed strong lattice preferred orientations with *c* axes parallel to the main compression axis of the DAC and *a* axes along the Be gasket plane, consistent with previous studies (Mao et al., 1998; Wenk et al., 2000) (Figs. 2 and 3). Here we calculated the sample densities (ρ) from the X-ray diffraction patterns collected in the axial geometry with an incident X-ray going through a diamond and diffracted signal going through another diamond (see Fig. 1 for the geometry) (Mao et al., 1998). The pressures of the sample were then calculated from the reported equation of state (EoS) (Mao et al., 1990). Energy spectra were collected by three avalanche photodiode detectors (APD) placed next to the DACs by tuning the X-ray energy to ±100 meV around the nuclear transition energy of 14.413 keV and collecting the Fe K-fluorescence radiation that was emitted with time delay. The energy spectra were measured at three different geometries at 158 (±5) GPa and 172 (±6) GPa, respectively, by rotating the textured hcp-Fe crystals in the meridian plane with respect to the incoming X-ray beam (Figs. 1 and 4). The probability of the inelastic nuclear absorption varies with the angle between the *k*-vector of the incident synchrotron radiation and the

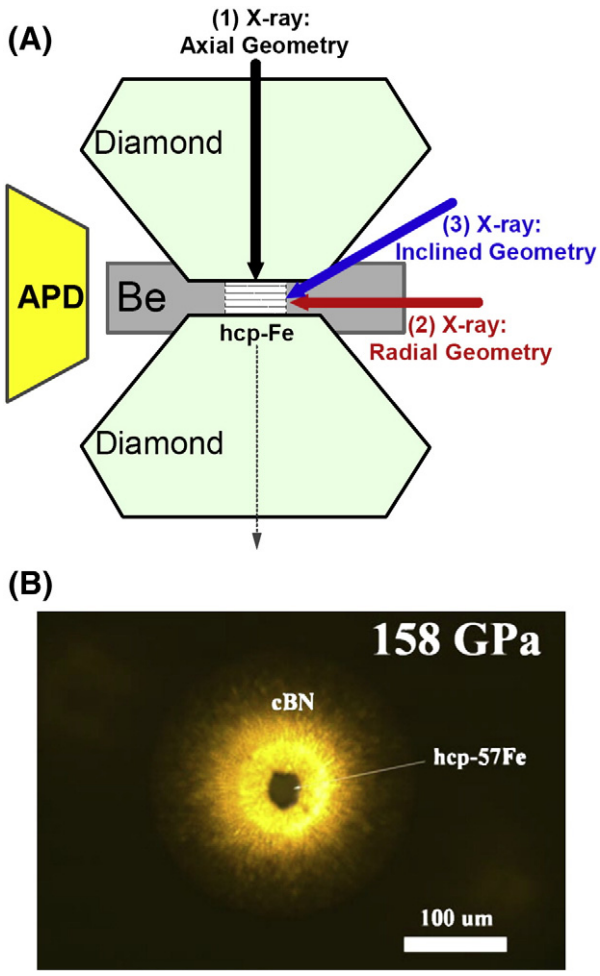

Fig. 1. (A) Schematics of the experimental geometries used for the NRIXS experiments with textured hcp-Fe in a DAC. (1). Axial geometry with an incident X-ray going through diamonds (black arrowed line); (2). radial geometry with an incident X-ray going through the Be gasket (red arrowed line); (3). inclined geometry with an incident X-ray tilted at 28° or 30° from the Be gasket (blue arrowed line). Three avalanche photodiode detectors (APD) were placed close to the Be gasket to detect the NRIXS signals. X-ray diffraction patterns were also measured along the axial and/or radial geometries. (B) Image of the textured hcp-Fe sample at 158 GPa and 300 K used for the experiments. The image was taken in transmitted light. Cubic BN was used as the gasket insert with the ultrapure Be gasket.

polarization vector of the excited or annihilated phonon, which allowed us to probe projected phonon density of states (DOS) along the direction of the incoming X-ray beam (Gieffers et al., 2002). The counting time for each spectrum was approximately 2 h, and approximately twenty spectra with a total of approximately 500 counts at the maximum of the inelastic energy spectra were collected and added for a given orientation.

3. Results

A quasi-harmonic model was used to extract the phonon DOS from the energy spectra (Fig. 5) and the Debye sound velocity (V_D) was derived from parabolic fitting of the low-energy regime of the DOS (Fig. 6) (Sturhahn, 2004). With the NRIXS technique we measure the spectrum of the self-correlation function of the position of the iron atoms (Sturhahn and Kohn, 1999). In the model, the atomic motions relative to the temperature-dependent averaged position are assumed to be harmonic under the given conditions of pressure, temperature, and other parameters. Thermal effects like expansion and change of force constants with atomic distances are allowed to

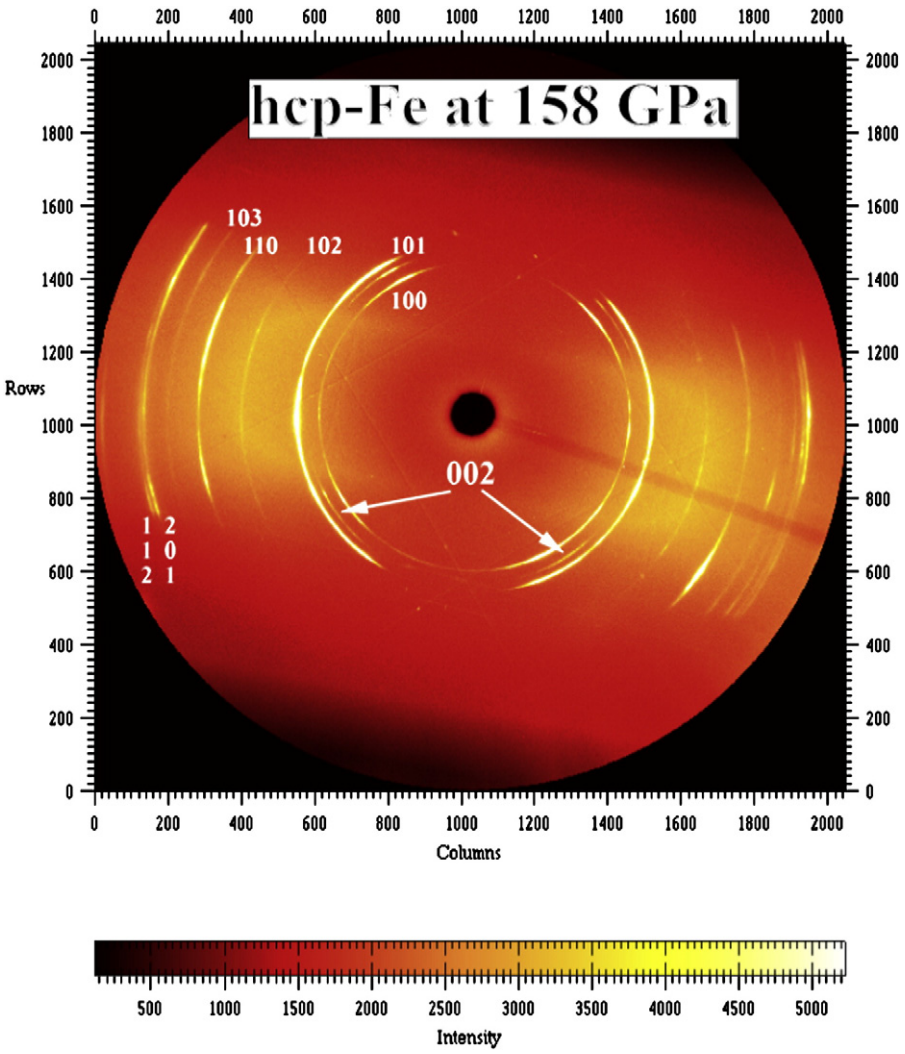

Fig. 2. Representative X-ray diffraction pattern of textured hcp-Fe sample at 158 GPa. hcp-Fe crystals displayed strong textures as a result of the non-hydrostatic compression. The pattern was taken through diamonds in the axial geometry (see Fig. 1(A) for the experimental geometry).

change but the vibrations are still assumed to occur in a harmonic potential (Sturhahn and Kohn, 1999). Previous studies have confirmed the reliability of this model to extract the phonon DOS and the V_D of iron under high pressures (Mao et al., 2001).

We used the PHOENIX program to analyze the energy spectra (Fig. 4), including determination of the elastic contribution to the spectra by matching the resolution function to the central peak and calculation of several moments of the spectra followed by normalization, removal of the elastic contribution from the data, decomposition into multi-phonon terms, and derivation of the DOS (Figs. 4–6). The high-quality energy spectra with an energy resolution of 1 meV is critical in allowing us to remove the elastic contribution very close to the low-energy region of the spectra and to extract phonon DOS for reliable derivations of the V_D needed to evaluate the Vs anisotropy of the textured hcp-Fe crystals. The V_D was derived using the parabolic fitting to the initial slope of the energy spectrum with the smallest chi-square distribution because the derivation of the V_D from the phonon DOS relies on a linear phonon dispersion that will only be accurate in a limited energy range which was approximately 22 meV in our analyses (Fig. 6; Table 1).

The derived V_D of hcp-Fe had been previously used with density and incompressibility values to solve for aggregate Vp, Vs, and shear modulus (G) averaged over randomly distributed crystals (e.g., Mao et al., 2001; Gieffers et al., 2002; Mao et al., 2004; Struzhkin et al., 2004; Lin et al., 2005; Mao et al., 2008). However, the equations for deriving these values become non-trivial and elaborated averaging schemes such as the Voigt–Reuss average or the Hashin–Shtrikman bounds are needed for a textured sample (Struzhkin et al., 2004). Nevertheless, the derived V_D is still very appropriate for deriving Vs because Vs can be generally expressed as $Vs = 0.952V_D - 0.041V_\Phi$ where V_Φ is the bulk sound velocity and only accounts for 4.1% of the contribution to the Vs. As addressed previously (Mao et al., 2004, 2008), Vs is very sensitive to V_D and a variation of V_Φ has only a very minor effect (~4% total in the expression) on the Vs, showing that Vs can be determined from the derived V_D with great precision and high accuracy (Fig. 7). We also used the literature adiabatic bulk modulus (Ks) values (Mao et al., 1990) to calculate the V_Φ ($V_\Phi^2 = Ks/\rho$). Our statistical error bars on the Vs, after taking the major source of uncertainty from the V_Φ into account, are on the order of 0.3 to 0.6% which is much smaller than the derived Vs anisotropy.

4. Discussion and conclusions

Systematic differences in the measured phonon DOS were observed from the textured hcp-Fe samples in the meridian plane at orientations projected along the *c* axes, *a* axes, and 28–30° to *a* axes (Fig. 7). For example, the derived mean force constant is systematically larger along the *c* axes than the *a* axes, indicating that the *c* axis is stiffer than the *a* axis. Of particular importance to the Vs anisotropy of the inner core is the variation of the V_D along different orientations

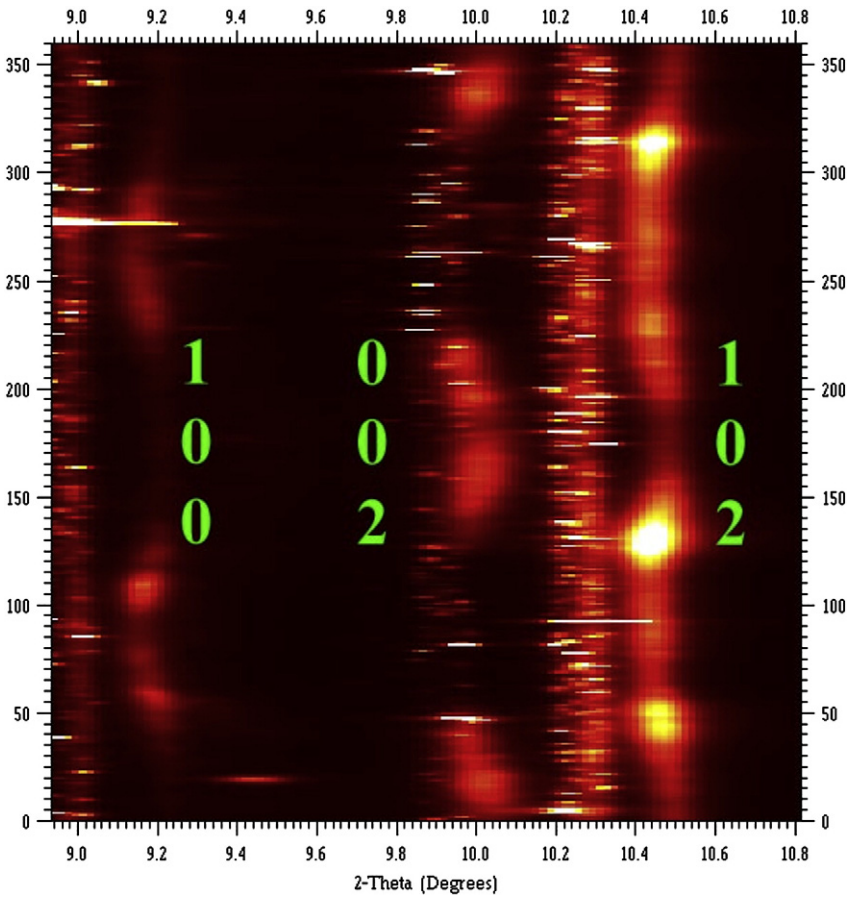

Fig. 3. Representative unrolled X-ray diffraction image of hcp-Fe sample at 158 GPa. The image was taken through a Be gasket in the radial geometry (see Fig. 1(A) for the experimental geometry). Representative X-ray diffraction lines of 100, 002, and 101 of the hcp-Fe show strong preferred orientation and strains. Green numbers next to unrolled diffraction lines represent Miller indices of the hcp-Fe diffraction peaks.

of the textured hcp-Fe crystals (Fig. 7). We note that our technique does not necessarily distinguish between polarized Vs_1 and Vs_2, and our Vs is averaged over Vs_1 and Vs_2 values intrinsically following the equation, $2/Vs^3 = 1/Vs_1^3 + 1/Vs_2^3$ (Mao et al., 2008; Struzhkin et al., 2004).

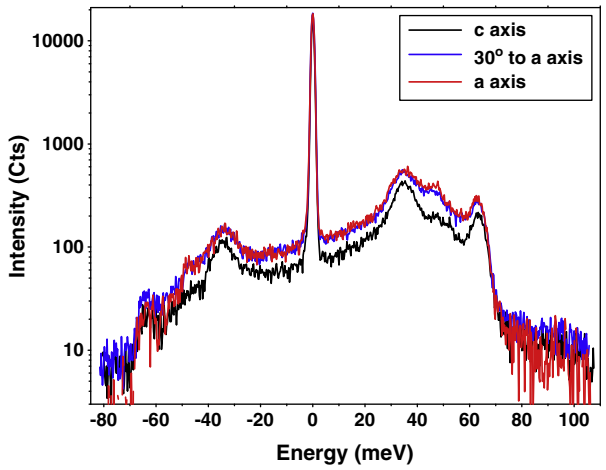

Fig. 4. Energy spectra of the hcp-Fe sample at 158 GPa. Three energy spectra were collected from the highly textured hcp-Fe sample along the *c* axis (black line), the *a* axis (red line), and 30° inclined to the *a* axis (blue line).

Our measured Vs vary systematically with the *c* axis being the fastest direction and the *a* axis the slowest direction. By defining the azimuthal Vs anisotropy as $2(V_{max}-V_{min})/(V_{max}+V_{min})$ where V_{max} is Vs along the *c* axis and V_{min} along the *a* axis from our measurements, the azimuthal Vs anisotropy is 4.1 (±0.7) % at 158 GPa and 1.5 (±0.8) % at 172 GPa (Fig. 7). Based on previous studies (Wenk et al., 2000), the preferred orientations in our hcp-Fe crystals should have fully developed at the investigated pressures (Fig. 3), indicating that the difference in Vs between 158 GPa and 172 GPa is likely a result of the statistical uncertainty, rather than the pressure effect alone. We thus conclude that the azimuthal Vs is 2–4% faster along the crystallographic *c* axis than along the *a* axis at 158 GPa and 172 GPa in the highly textured hcp-Fe. Combined with a previous experimental study on the Vp anisotropy of textured hcp-Fe crystals (Antonangeli et al., 2004), the Vp anisotropy qualitatively exhibits a similar sigmoidal shape to the Vs anisotropy. Compared with previous studies for hcp-Fe at relevant pressure conditions, our observed azimuthal Vs anisotropy of 2–4% at 158–172 GPa is consistent with that of Laio et al. (2000) but much lower than other reports (e.g., Mao et al., 1998; Laio et al., 2000; Steinle-Neumann et al., 1999, 2001; Sha and Cohen, 2010) (Fig. 8). Because our Vs anisotropy is measured from the highly textured hcp-Fe at room temperature, the azimuthal anisotropy for individual Vs_1 and Vs_2 of a single-crystal hcp-Fe is expected to be different. Furthermore, high temperature and higher pressures may further affect the magnitude of the anisotropy (e.g., Lin et al., 2005; Vocadlo et al., 2009; Sha and Cohen, 2010).

A shear wave splitting anisotropy of approximately 1% in the inner core has been recently invoked to explain the waveform features and

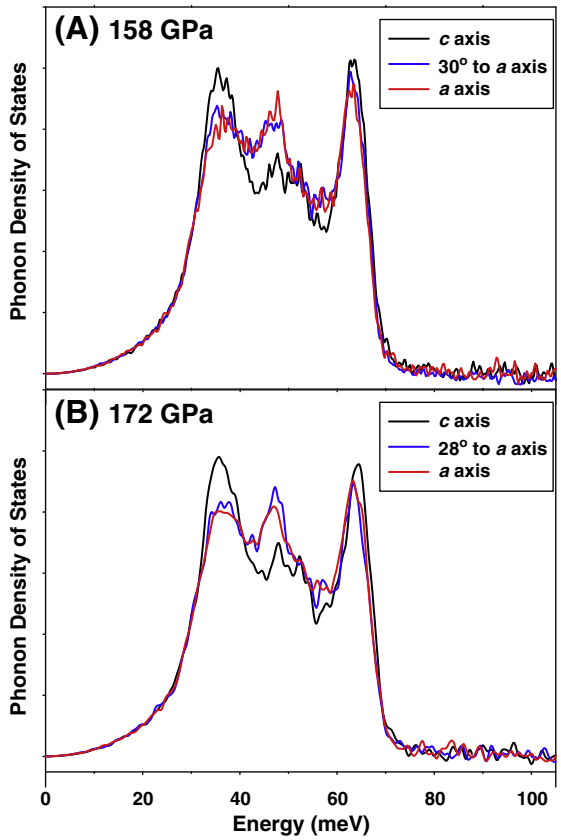

Fig. 5. Phonon density of states (DOS) of textured hcp-Fe at 158 GPa. The DOS were derived from the measured energy spectra along three different directions, and were used to derive Debye sound velocities (V_D) and shear wave velocities (Vs) (Fig. 7). The black line represents the phonon DOS measured along the compression axis of the DAC (along the *c* axes of the hcp-Fe crystals). The red line represents the phonon DOS along the *a* axes (along the Be gasket), whereas a third orientation with 30° at 158 GPa or 28° at 172 GPa inclined to the *a* axes (blue line) was also probed (see Fig. 1(A) for the experimental geometries).

to reconcile the large differences between the Vp and attenuation models for an inner-core shear wave phase at higher frequencies (Wookey and Helffrich, 2008). If one describes the Vp anisotropy of the inner core by the existence of the textured hcp-Fe crystals (e.g.,

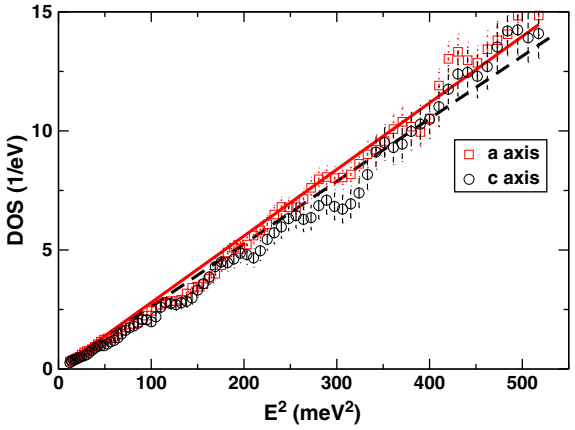

Fig. 6. Representative derivation of the V_D from the phonon DOS at 158 GPa. The derived V_D clearly showed that it is faster along the *c* axis than along the *a* axis. Black open circles: the phonon DOS measured along the *c* axes of the hcp-Fe crystals; red open squares: the phonon DOS along the *a* axes.

Table 1
Derived Debye sound velocities (V_D), shear wave velocities (Vs), and mean force constants (D_{av}) of hcp-Fe at three orientations at 158 GPa ($\rho = 12.159$ g/cm^3 (± 0.068)) and 172 GPa ($\rho = 12.338$ g/cm^3 (± 0.069)), respectively. The mean force constants are directly derived from the measured energy spectra.

File	V_D (km/s)	V_S (km/s)	D_{av} (mm/s)
158 GPa; *c* axis	5.833 ($\pm$0.033)	5.213 ($\pm$0.031)	511.7 ($\pm$5.6)
158 GPa; 30° to *a* axis	5.691 ($\pm$0.027)	5.080 ($\pm$0.025)	508.1 ($\pm$3.5)
158 GPa; *a* axis	5.615 ($\pm$0.024)	5.009 ($\pm$0.023)	491.1 ($\pm$4.5)
172 GPa; *c* axis	5.848 ($\pm$0.036)	5.222 ($\pm$0.034)	531.4 ($\pm$8.8)
172 GPa; 28° to *a* axis	5.742 ($\pm$0.041)	5.124 ($\pm$0.038)	534.5 ($\pm$7.7)
172 GPa; *a* axis	5.714 ($\pm$0.031)	5.098 ($\pm$0.029)	526.8 ($\pm$8.8)

Tromp, 1993; Wenk et al., 2000; Vocadlo et al., 2009), the azimuthal and polarized Vs anisotropies of a few percent in magnitude need to be invoked for the region (Wookey and Helffrich, 2008), likely with Vp and Vs traveling faster along the rotation axis of the Earth than along the equatorial direction (Antonangeli et al., 2004). Since Vp and Vs anisotropies of hcp-Fe and bcc-Fe can behave quite differently at high pressures and temperatures, future high-resolution seismic observations of the Vs and Vp anisotropies thus hold the key to deciphering the underlying causes for the seismic heterogeneities and dynamic mechanisms of the inner core.

Acknowledgments

We acknowledge XOR-3 and GSECARS of the Advanced Photon Source (APS) at the Argonne National Laboratory (ANL) for providing synchrotron and optical facilities. We appreciate H. Scott, V.V.

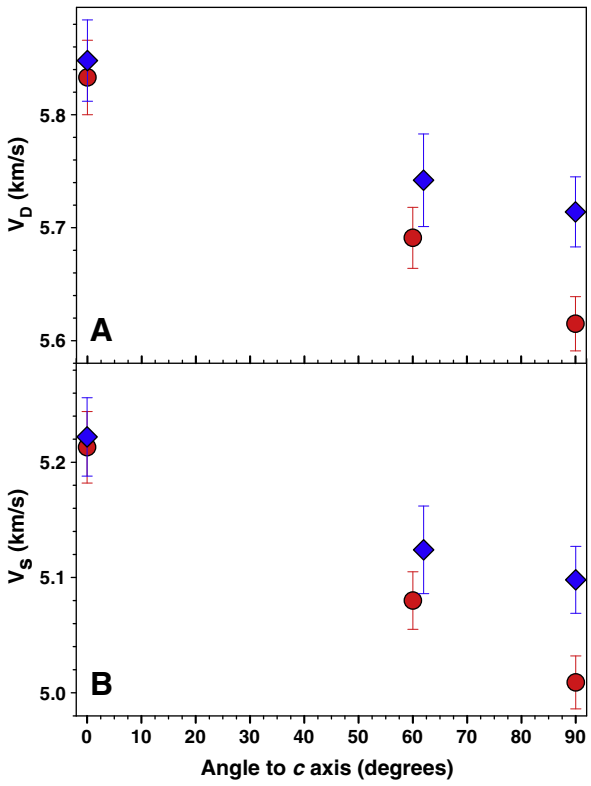

Fig. 7. Debye sound velocities (V_D) and shear wave velocities (Vs) of textured hcp-Fe. Red circles: 158 GPa; blue diamonds: 172 GPa. The error bars on the V_D and Vs are approximately 0.4–0.7%, which are much smaller than the observed anisotropies.

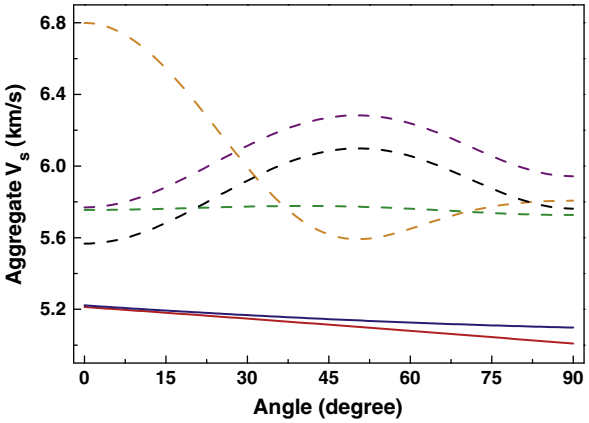

Fig. 8. Comparison of azimuthal shear wave velocities of hcp-Fe. For simplicity, representative theoretical calculations under similar conditions to our experiments are plotted for comparison (Mao et al., 1998; Steinle-Neumann et al., 1999; Laio et al., 2000; Sha and Cohen, 2010). The Vs were calculated from the polarized Vs_1 and Vs_2 values using the expression, $2/Vs^3 = 1/Vs_1^3 + 1/Vs_2^3$, similar in scheme to our measured Vs values. The angle at 0° is parallel to the *c* axis of the hcp-Fe, whereas the angle at 90° represents the *a* axis of the hcp-Fe. Our experimental results at 158 GPa ($\rho = 12.159$ g/cm^3 (± 0.068)) (red line) and 172 GPa ($\rho = 12.338$ g/cm^3 (± 0.069)) (blue line) are represented by a simple second-order polynomial function. Purple dashed lines: hcp-Fe at 12.47 g/cm^3 and 0 K (Steinle-Neumann et al., 1999); green dashed lines: hcp-Fe at 12.5 g/cm^3 and 300 K (Laio et al., 2000); black dashed lines: hcp-Fe at 12.52 g/cm^3 and 300 K (Sha and Cohen, 2010). Experimental results derived from previous RXD data (orange dashed lines) (Mao et al., 1998) for hcp-Fe at 12.61 g/cm^3 (211 GPa) and 300 K are also plotted for comparison.

Prapapenka and I. Kantor for their assistance in X-ray diffraction experiments. APS is supported by DOE-BES, under Contract No. DE-AC02-06CH11357. J.F.L. and Z.M. acknowledge support from the US National Science Foundation (EAR-0838221), Energy Frontier Research at Extreme Environments (EFree) of the Energy Frontier Research Centers (EFRCs), and the Carnegie/DOE Alliance Center (CDAC). H.Y. was supported by COMPRES, the Consortium for Materials Properties Research in Earth Sciences under NSF Cooperative Agreement EAR 06-49658. We thank E.E. Alp, W. Sturhahn, S. Grand, E. Garnero, and C. Jacobs for helpful discussions.

References

Antonangeli, D., Occelli, F., Requardt, H., Badro, J., Fiquet, G., Krisch, M., 2004. Elastic anisotropy in textured hcp-iron to 112 GPa from sound wave propagation measurements. Earth Planet. Sci. Lett. 225, 243–251.

Antonangeli, D., Merkel, S., Farber, D.L., 2006. Elastic anisotropy in hcp metals at high pressure and the sound wave anisotropy of the Earth's inner core. Geophys. Res. Lett. 33, L24303. doi:10.1029/2006GL028237.

Beghein, C., Trampert, J., 2003. Robust normal mode constraints on inner-core anisotropy from model space search. Science 299, 552–555.

Belonoshko, A.B., Skorodumova, N.V., Davis, S., Osiptsov, A.N., Rosengren, A., Johansson, B., 2007. Origin of the low rigidity of the Earth's inner core. Science 316, 1603–1605.

Belonoshko, A.B., Skorodumova, N.V., Rosengren, A., Johansson, B., 2008. Elastic anisotropy of Earth's inner core. Science 319, 797–800.

Cao, A., Romanowicz, B., 2009. Constraints on shear wave attenuation in the Earth's inner core from an observation of PKJKP. Geophys. Res. Lett. 36, L09301.

Cao, A.M., Romanowicz, B., Takeuchi, N., 2005. An observation of PKJKP: inferences on inner core shear properties. Science 308, 1453–1455.

Creager, K.C., 1997. Inner core rotation rate from small-scale heterogeneity and time-varying travel times. Science 278, 1284–1288.

Deuss, A., 2008. Normal mode constraints on shear and compressional wave velocity of the Earth's inner core. Earth Planet. Sci. Lett. 268, 364–375.

Dubrovinsky, L., Lin, J.F., 2009. Mineral physics quest to the Earth's core. Eos. Trans. Am. Geophys. Union 90 (3), 21–28.

Dubrovinsky, L., Dubrovinskaia, N., Narygina, O., Kantor, I., Kuznetzov, A., Prakapenka, V.B., Vitos, L., Johansson, B., Mikhaylushkin, A.S., Simak, S.I., Abrikosov, I.A., 2007. Body-centered cubic iron–nickel alloy in Earth's core. Science 316, 1880–1883.

Gieffers, H., Lubbers, R., Rupprecht, K., Wortmann, G., Alfe, D., Chumakov, A.I., 2002. Phonon spectroscopy of oriented hcp iron. High Pressure Res. 22, 501–506.

Hemley, R.J., Mao, H.K., 2001. *In situ* studies of iron under pressure: new windows on the Earth's core. Int. Geol. Rev. 43, 1–30.

Ishii, M., Dziewonski, A., 2002. The innermost inner core of the earth: evidence for a change in anisotropic behavior at the radius of about 300 km. Proc. Natl Acad. Sci. 99, 14026–14030.

Laio, A., Bernard, S., Chiarotti, G.L., Scandolo, S., Tosatti, E., 2000. Physics of iron at Earth's core conditions. Science 287, 1027–1030.

Li, L., Fei, Y., 2003. Experimental constraints on core composition. Treatise Geochem. 2, 521–546.

Lin, J.F., Sturhahn, W., Zhao, J., Shen, G., Mao, H.K., Hemley, R.J., 2005. Sound velocities of hot dense iron: Birch's law revisited. Science 308, 1892–1894.

Lin, J.F., Watson, H.C., Vankó, G., Alp, E.E., Prakapenka, V.B., Dera, P., Struzhkin, V.V., Kubo, A., Zhao, J., McCammon, C., Evans, W.J., 2008. Intermediate-spin ferrous iron in lowermost mantle post-perovskite and perovskite. Nat. Geosci. 1, 688–691.

Lin, J.F., Mao, Z., Jarrige, I., Xiao, Y., Chow, P., Okuchi, T., Hiraoka, N., Jacobsen, S.D., 2010. Resonant X-ray emission study of the lower-mantle ferropericlase at high pressures. Am. Miner. 95, 1125–1131.

Mao, H.K., Wu, Y., Chen, L.C., Shu, J., 1990. Static compression of iron to 300 GPa and $Fe_{0.8}Ni_{0.2}$ alloy to 260 GPa: implications for composition of the core. J. Geophys. Res. 95, 21737–21742.

Mao, H.K., Shu, J., Shen, G., Hemley, R.J., Li, B., Singh, A.K., 1998. Elasticity and rheology of iron above 220 GPa and the nature of the Earth's inner core. Nature 396, 741–743.

Mao, H.K., Xu, J., Struzhkin, V.V., Shu, J., Hemley, R.J., Sturhahn, W., Hu, M.Y., Alp, E.E., Vocadlo, L., Alfe, D., Price, G.D., Gillan, M.J., Schwoerer-Bohning, M., Hausermann, D., Eng, P., Shen, G., Giefers, H., Lubbers, R., Wortmann, G., 2001. Phonon density of states of iron up to 153 gigapascals. Science 292, 914–916.

Mao, W.L., Sturhahn, W., Heinz, D.L., Mao, H.K., Shu, J., Hemley, R.J., 2004. Nuclear resonant X-ray scattering of iron hydride at high pressure. Geophys. Res. Lett. 31, L15618. doi:10.1029/2004GL020541.

Mao, W.L., Struzhkin, V.V., Baron, A.Q.R., Tsutsui, S., Tommaseo, C.E., Wenk, H.R., Hu, M. Y., Chow, P., Sturhahn, W., Shu, J., Hemley, R.J., Heinz, D.L., Mao, H.K., 2008. Experimental determination of the elasticity of iron at high pressure. J. Geophys. Res. 113, B09213.

Morelli, A., Dziewonski, A.M., Woodhouse, J.H., 1986. Anisotropy of the inner core inferred from *PKIKP* travel times. Geophys. Res. Lett. 13, 1545–1548.

Niu, F., Chen, Q.F., 2008. Seismic evidence for distinct anisotropy in the innermost inner core. Nature Geosci. 1, 692–696.

Sha, X., Cohen, R.E., 2010. Elastic isotropy of ε-Fe under Earth's core conditions. Geophys. Res. Lett. 37, L10302. doi:10.1029/2009GL042224.

Singh, A.K., Balasingh, C., Mao, H.K., Hemley, R.J., Shu, J., 1998. Analysis of lattice strains measured under non-hydrostatic pressure. J. Appl. Phys. 83, 7567–7575.

Song, X., Helmberger, D.V., 1998. Seismic evidence for an inner core transition zone. Science 282, 924–927.

Song, X.D., Helmburger, D.V., 1993. Anisotropy of Earth's inner core. Geophys. Res. Lett. 20, 2591–2594.

Steinle-Neumann, G., Stixrude, L., Cohen, R.E., 1999. First-principles elastic constants for the hcp transition metals Fe, Co, and Re at high pressure. Phys. Rev. B 60, 791–799.

Steinle-Neumann, G., Stixrude, L., Cohen, R.E., Gulseren, O., 2001. Elasticity of iron at the temperature of the Earth's inner core. Nature 413, 57–60.

Stixrude, L., Cohen, R.E., 1995. High-pressure elasticity of iron and anisotropy of Earth's inner core. Science 267, 1972–1975.

Struzhkin, V.V., Hemley, R.J., Mao, H.K., 2004. New condensed matter probes for diamond anvil cell technology. J. Phys. Condens. Matter 16, S1071–S1086.

Sturhahn, W., 2004. Nuclear resonant spectroscopy. Matter. J. Phys.: Condens 16, S497–S530.

Sturhahn, W., Kohn, V.G., 1999. Theoretical aspects of incoherent nuclear resonant scattering. Hyperfine Interact. 123 (124), 367–399.

Takahashi, T., Bassett, W.A., 1964. A high pressure polymorph of iron. Science 145, 483–486.

Tromp, J., 1993. Support for anisotropy of the Earth's inner core from free oscillations. Nature 366, 678–681.

Vocadlo, L., 2007. *Ab* initio calculations of the elasticity of iron and iron alloys at inner core conditions: evidence for a partially molten inner core? Earth Planet. Sci. Lett. 254, 227–232.

Vocadlo, L., Alfè, D., Gillan, M.J., Wood, I.G., Brodholt, J.P., Price, G.D., 2003. Possible thermal and chemical stabilization of body-centred-cubic iron in the Earth's core. Nature 424, 536–539.

Vocadlo, L., Dobson, D.P., Wood, I.G., 2009. *Ab* initio calculations of the elasticity of hcp-Fe as a function of temperature at inner-core pressure. Earth Planet. Sci. Lett. 288, 534–538.

Wenk, H.-R., Matthies, S., Hemley, R.J., Mao, H.K., Shu, J., 2000. The plastic deformation of iron at pressures of the Earth's inner core. Nature 405, 1044–1047.

Woodhouse, J.H., Giardini, D., Li, X.D., 1986. Evidence for inner core anisotropy from free oscillations. Geophys. Res. Lett. 1549–1552.

Wookey, J., Helffrich, G., 2008. Inner-core shear-wave anisotropy and texture from an observation of PKJKP waves. Nature 454, 873–877.